ARID ZONE JOURNAL OF ENGINEERING, TECHNOLOGY & ENVIRONMENT
AZOJETE December 2025. Vol.21(4):1012-1025
Published by the Faculty of Engineering, University of Maiduguri, Maiduguri, Nigeria.
Print ISSN: 1596-2490, Electronic ISSN: 2545-5818
https://doi.org/10.63958/AZOJETE/2025/21/04/011
www.azojete.com.ng

ORIGINAL RESEARCH ARTICLE

AN ENHANCED AQUILA OPTIMIZER-BASED DISTRIBUTED GENERATION FRAMEWORK FOR HARMONIC MITIGATION

I.M. Adeyinka[1], I. Abubakar[1], N.B. Kadandani[1,2] and M.M. Sa'ad[3]

[1]*Department of Electrical Engineering, Bayero University, PMB 3011, Kano, Nigeria.*
[2]*Department of Electrical and Electronics Engineering, Federal University of Transportation, PMB 1050, Daura, Katsina State, Nigeria.*
[3]*Department of Electrical and Electronics Engineering, Veritas University, Abuja, Nigeria.*
Corresponding author's email: muyik78@yahoo.com

ARTICLE INFORMATION

Received: 16th October 2025
Revised: 12th November 2025
Accepted: 13th November 2025

Keywords:
Improved aquila optimizer
Aquila optimizer
Adaptive grey wolf optimizer
Total harmonic distortion
Active power filter

ABSTRACT

This research work presents an improved Aquila optimizer-based distributed generation system for solving power quality problems. This is particularly important for mitigating the harmonics presence in a radial distribution system (RDS). The radial distribution network (RDN) was modeled in the presence of the nonlinear load (NLLD) and nonlinear distributed generation (NLDG). RDN provides a simple, cost-effective structure with a single power source that can be analyzed with a simplified forward/backward sweep load flow algorithm, making it easier to determine the optimal size and location of active power filters to mitigate harmonics and improve voltage quality. An improved Aquila optimization algorithm was then used to optimally size and place active power filters (APFs) in the adaptive RDN to control the harmonics, ensuring that the harmonics present in the system do not exceed IEEE-519 of 1992 standard limits. The results obtained from the developed scheme were presented and compared with the results obtained when Adaptive Grey Wolf Optimizer (AGWO) and Aquila Algorithm (AO) were used. THD and fitness function were used as the performance metrics. All simulations were carried out in the MATLAB/Simulink environment R2022b. The THD values obtained during various periods of the day were presented and it was observed that high distortions were recorded between hours 11 to 13, with the highest distortion occurring at hour 12. To further analyze the efficacy of the developed approach after placement of the APF in the IEEE 69-bus network, the result of the THD obtained when the improved Aquila algorithm was used for the placement of the APFs were presented. It was observed that the THD values obtained for the entire 69-bus network were well within the IEEE standard limit. Further, the results obtained from the developed scheme were compared with those obtained when AGWO and AO were used for harmonic mitigation in the distribution system. It was observed that the THD values obtained by the developed scheme outperformed those obtained from the AGWO technique by 5.96%, 4.71%, 3.47%, 32.79%, 3.62%, 11.68%, and 30.25%, respectively, for the bus numbers that have higher distortion values, while it also outperformed the Aquila algorithm by 3.07%, 2.41%, 1.88%, 31.97%, 1.84%, 16.88%, and 25.98%, respectively. The developed approach provides a practical and computationally efficient solution for harmonic mitigation and can be extended to larger and more complex power systems for improved grid performance.

1.0 Introduction

Electricity is an indication of convenience life, and the demand for this energy source is increasing. Development in the power industry has led to a rise in both linear and nonlinear loads within power systems. Many solid-state switching converters consume reactive power and generate current harmonics from the AC

grid, contributing to total harmonic distortion in voltage (THDv) and current (THDi) under nonlinear load conditions (Abbas *et al*., 2021). In modern power systems, the increasing penetration of distributed generation (DG) units particularly those interfaced through power electronics has introduced complex power quality challenges such as voltage instability, harmonic distortion, elevated thermal losses due to heat loss (I^2R), and reactive power imbalance. These issues degrade the efficiency and reliability of radial distribution networks, especially under dynamic and nonlinear operating conditions.

The growing integration of distributed generation (DG) units, especially those using power electronic interfaces, has therefore introduced significant power quality issues in radial distribution networks. These include harmonic distortion, voltage instability, increased thermal losses, and reactive power imbalance all of which compromise system efficiency and reliability under nonlinear and dynamic conditions. While Aquila Optimizer-based DG placement has been shown to effectively reduce real power losses and enhance voltage profiles, it lacks mechanisms for harmonic suppression and reactive power management. Moreover, the unpredictable output of DGs and the nonlinear behavior of inverter-based sources further intensify these challenges. To address these limitations, this research proposes the incorporation of an Active Power Filter (APF) into the Aquila-optimized DG framework. The APF actively mitigates harmonics and compensates reactive power, forming a hybrid solution that improves voltage stability, reduces distortion, and enhances overall energy efficiency ultimately boosting the resilience and sustainability of distributed radial networks. These nonlinear loads generate harmonics that cause disturbances and can lead to system malfunction. Today, almost every modern equipment, power system, and service such as furnaces, computer power supplies, communication systems, renewable energy systems, electrical power generation, and high-voltage systems—requires a continuous and high-quality power supply. Consequently, researchers and utility companies continue to explore solutions to power quality problems (Sakar *et al*., 2017), including harmonics, voltage fluctuation, voltage sag, unbalance, frequency variation, and transient spikes. The increasing proliferation of nonlinear loads worsens harmonic distortion in the power system, resulting in degraded power quality.

Flexible AC Transmission System (FACTS) devices such as Static Compensators (STATCOMs) and Active Power Filters (APFs) have emerged as dominant technologies for mitigating these issues in industrial and commercial systems. In radial distribution networks (RDN), nonlinear loads (NLLDs) and nonlinear distributed generations (NLDGs) are the primary sources of harmonics, which elevate both the individual and total harmonic distortion in voltage (THDv). The degradation of electrical power quality due to multiple nonlinear loads—such as rectifiers, uninterruptible power supplies (UPS), and various electronic circuits leads to low power factor, poor energy efficiency, and voltage distortion (Sakar *et al*., 2017; Battu et al., 2015; Uniyal & Kumar, 2018). The inclusion of a shunt active power filter (SAPF) and photovoltaic (PV) system represents an effective solution for harmonic reduction and reactive power compensation, ensuring an improved power factor correction (PFC) at the point of common coupling (PCC).

Metaheuristic optimization techniques such as Genetic Algorithm (GA), Ant Colony Optimization (ACO), Bee Colony Optimization, and Particle Swarm Optimization (PSO) have gained popularity due to their simplicity, flexibility, derivation-free mechanisms, and avoidance of local optima (Mirjalili & Lewis, 2016). Among recent advances, the Aquila Optimizer (AO) a nature-inspired algorithm based on the hunting behavior of the Aquila bird (Dhal *et al*., 2024) has demonstrated remarkable performance in solving complex nonlinear optimization problems. Similarly, the Grey Wolf Optimizer (GWO), inspired by the leadership hierarchy and hunting mechanism of grey wolves, has shown competitive performance when benchmarked against well-known metaheuristic algorithms such as PSO, Gravitational Search Algorithm (GSA), Differential Evolution (DE), and Evolutionary Programming (EP) (Mirjalili & Lewis, 2016).

Previous works have explored various approaches for harmonic mitigation and optimal placement of filters or DG units. For instance, (Sakar *et al*., 2017) determined hosting capacity for distorted systems with PV-based DGs under harmonic constraints, while (Fahmi *et al.,* 2018) utilized a single-tuned passive filter to reduce harmonics in industrial systems. However, passive filters are inadequate for complex, nonlinear environments. (Lakum & Mahajan, 2019) examined the impact of DG penetration on APF placement using the GWO algorithm, revealing that DG integration significantly affects APF sizing. Moreover, (Abbas *et al.,* 2021) used a Water Cycle Algorithm (WCA) to plan single-tuned filters for inverter-based DGs, reducing THD effectively but without addressing adaptive compensation under nonlinear dynamics. From these reviewed studies, it is evident that determining the optimal placement and sizing of APFs remains crucial for minimizing cost while maintaining high power quality in RDNs. The introduction of DG converters brings additional harmonic challenges that necessitate more adaptive mitigation strategies. Hence, this work presents an improved Aquila Optimizer-based approach for optimal APF placement and sizing, aiming to reduce power losses, enhance

Corresponding author's email address: muyik78@yahoo.com

voltage profiles, and effectively suppress harmonics thereby improving the overall stability and efficiency of radial distribution networks.

2. Materials and Method

This section presents the comprehensive methodology employed in this paper. It provides detail of the mathematical model of the system, the formulation of the objective function used to evaluate performance of the algorithm.

2.1 Modeling of the Radial Distribution Network

The radial distribution network employed is represented as a branch impedance (Z_{ab}) which is expressed in equation 1 (Lakum & Mahajan, 2021).

$$\mathbf{Z_{a,b} = R_{a,b} + jX_{L,a,b}} \quad 1$$

Where Zab is the impedance between line a to b, R_{ab} is the resistance between line a to b, X_{Lab} is the reactance between line a to b.

The graphical modeling of the RDS with the NLDGs, harmonic filters and nonlinear loads developed in MATLAB Simulink is as shown in Figure 1.

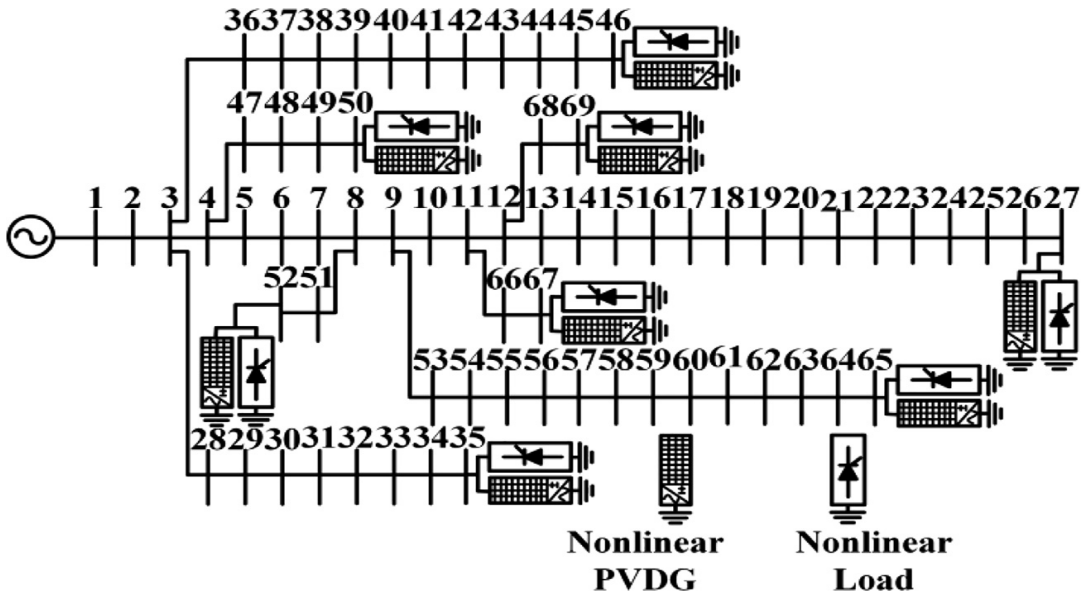

Figure 1: IEEE 69- Bus System with Nonlinear Loads and NLDGs (Lakum & Mahajan, 2021)

As the RDN contains NLDGs and nonlinear loads, the branch impedance equation must be modified to include harmonics. As such the expression for the branch impedance can now be expressed as in equations 2 to 4:

$$\mathrm{Z_{a,b}^{(h)} = R_{a,b} + jX_{L,a,b}^{(h)}} \quad 2$$

$$\mathrm{X_{L,a,b}^{(h)} = \omega_h L_{a,b}} \quad 3$$

$$\mathrm{\omega_h = 2\pi f_h} \quad 4$$

where Z is the equivalent impedance of the system a and b, represent the bus numbers, h represents the order of harmonics, $R_{a,b}$ depicts the resistances of branch ab, f_h represents the harmonic frequency of the current, $L_{a,b}$ denotes the inductance of branch ab and ω_h represents the angular frequency of the harmonic current.

2.2 Mathematical model of RDS with NLLD

The nonlinear loads are modeled as harmonic current injection source and their rms value is given in equations 5 and 6. The harmonic current $I_{nl,a}^{(h)}$ at harmonic h is represented as a complex number, with real and imaginary parts:

$$I_{nl,a}^{(h)} = I_{nl,a,r}^{(h)} + jI_{nl,a,im}^{(h)} \quad 5$$

$$I_{nl,a}^{(h)} = \sqrt{\sum_{h=2}^{H} (I_{nl,a,r}^{2(h)} + I_{nl,a,im}^{2(h)})} \quad 6$$

where $I_{nl,r}^{(h)}$ and $I_{nl,im}^{(h)}$ represent the real and imaginary parts of the load current repectively. $I_{nl,a}^{(h)}$ depicts the rms value for the nonlinear load current at bus "a", while H represents the highest order of harmonics.

2.3 Mathematical Model of RDS with NLDG

Since the NLDG is in charge of introducing nonlinear current into the system, it is modeled as a current source in this work. The fundamental current is determined by the DG's power rating, and the DG's nonlinear harmonic current value can be obtained by using the expression in equation 7 in accordance with the harmonic spectrum.

$$I_{nldg,a}^{(h)} = K_{dg} I_{dg,a} \quad 7$$

where $I_{nldg,a}^{(h)}$ is the harmonic current of the DG, while K_{dg} depicts the percentage of harmonic current as per the harmonic spectrum of DG, lastly $I_{dg,a}$ is the fundamental current of DG.

2.4 APF Modeling

The APF is modeled as a current source. The calculation of the APF current is done on the basis of net nonlinear which is a vector addition of nonlinear currents of loads and NLDGs. When the phase angle is zero, the distortion is worst as the net nonlinear current is a function of phase angle. So it causes maximum distortion while harmonic currents are in phase;

$$I_{nldg}^{(h)} = I_{hdg}^{(h)} + I_{nl}^{(h)} \quad 8$$

$$I_{apf} = k(I_{nldg}) \quad 9$$

where k is proportionate to net nonlinear current. Since APF is represented as a set of current sources. It injects harmonics order at a point of common coupling (PCC) as per the value of k. the APF can be expressed as:

$$I_{apf}^{(h)} = I_{apf,r}^{(h)} + jI_{apf,im}^{(h)} \quad 10$$

$$I_{apf} = \sqrt{\sum_{h=2}^{H} \{I_{apf,r}^{2(h)} + I_{apf,im}^{2(h)}\}} \quad 11$$

where $I_{apf,r}^{2(h)}$ represents the real part of the APF, while $I_{apf,im}^{2(h)}$and I_{apf} depicts the imaginary part and rms value of current of the APF respectively.

2.5 Modeling of Solar Power Generation

It is evident that the power output from solar PV is proportional to the irradiance. The solar PV output power can be calculated as shown in equation 12.

$$P_{pv}(si) = \eta^{pv} \times S^{pv} \times si \quad 12$$

where, P_{pv} represents the output power in kW, S^{pv} denotes the total area of PV in meter square and η^{pv} represents the efficiency.

Normal probability density function is used in this work to generate the samples of the output power of the solar power plant. A k-means scenario reduction algorithm is employed to reduce the number of samples (output power of the solar PV) to 100. The reduced samples were then used to calculate the harmonic currents injected by the NLDG.

Corresponding author's email address: muyik78@yahoo.com

2.6 Harmonic Load Flow

In this study, a harmonic load flow based on network topology is used. Two matrices are created in this approach: bus injection to branch current (BIBC), and branch current to the bus voltage (BCBV). With harmonic load flow, the THDv is computed at each bus. It is necessary to identify the crucial busses that go beyond the accepted bounds. The THDv equation is represented as:

$$\mathrm{THD_v} = \frac{\sqrt{\sum_{h=2}^{H}(\mathrm{IHDv})^2}}{V_f^1} \quad 13$$

where the fundamental frequency voltage is denoted with V_f^1. From the value of THDv at all buses, the vital buses where the IEEE standard limits are not satisfied are found. It helps to decide the policy to alleviate the harmonics which in this research is the placement and sizing of APF.

2.7 Objective Function

The objective function formulated is subject to satisfying the following constraints:

$$THD_v \leq 5\% \quad 14$$

$$IHD_v \leq 3\% \quad 15$$

$$I_{apf} \leq I_{apf,max} \quad 16$$

Where $I_{apf,max}$ represents the maximum current of APF and DP represents the dynamic penalty. The value set in the constraints for the THD_v and IHD_I are selected to ensure that the requirement of IEEE standard 519 are met.

2.8 Extended Nonlinear Load Position Base APF Current Injection Formulation

Formulation of the extended NLPCI is done in this sub-section. The extended NLPCI is used to find the optimal buses for placement of APF in the RDS. The proposed technique consists of three cases: a) only one feasible state with a minimum number of APF, b) more than one state with same number of APFs with different THDv, and c) more than one state with same number of APF and same THDv. NLPCI technique has been introduced to decide the feasible buses for the entire 33-bus RDS.

Create the nonlinear load position based APF placement matrix:

The total number of nonlinear load is denoted by NL and its buses is denoted by B NL.

Then nonlinear loads are represented as, matrix of [1 0 0 0,…,…NL]

The nonlinear load buses are represented as, matrix of [1 0 0 0,…,... $B_{\mathbf{NL}}$]. The nonlinear load position based matrix is formed and possible combinations of APFs placement are calculated. Each combination comprises of a set of nonlinear load buses and it is denoted by state St. Number of total state ST is determined from nonlinear load buses as:

$$ST = 2^{NL} - 1 \quad 17$$

The nonlinear load position based APF placement combination matrix of zeros and 1

here, '1' represents the placement of APF and '0 represents no APF.

Form the set of feasible states SF:

APF with an equal rating of the nonlinear load is connected at possible combination i.e., each state. Then THDv is calculated at all the buses using harmonic load flow for all the states. According to their maximum THDv the states are denoted as,

$St_{1\,THDV\ max}$; ……, ….. ,$ST_{\ THDV\ max.}$

Separation of feasible and infeasible state is done by fulfilling the standard limit of THDv as,

Corresponding author's email address: muyik78@yahoo.com

$$\text{State S} = \begin{Bmatrix} \text{SF}, \text{St}_{\text{THD}_v\max} \leq 5\% \\ \text{infeasible}, \text{St}_{\text{THD}_v\max} > 5\% \end{Bmatrix} \quad 18$$

Form the group according to the number of APFs:

All the states are arranged as per their number of filters. Here, the total nonlinear load buses are NL. Therefore, the maximum possible combination according to the number of APFs is decided by

NLC $_{\text{Nft}}$. $G_{Nft}\{SF_{Nft}\}$ $(Group\ with\ maximum\ filter)$.

The group with the maximum number of APFs has only one state.

This technique is extended here and formulated as follows: The steps employed in ensuring efficient operation of the extended NLPCI is as shown in the flowchart below:

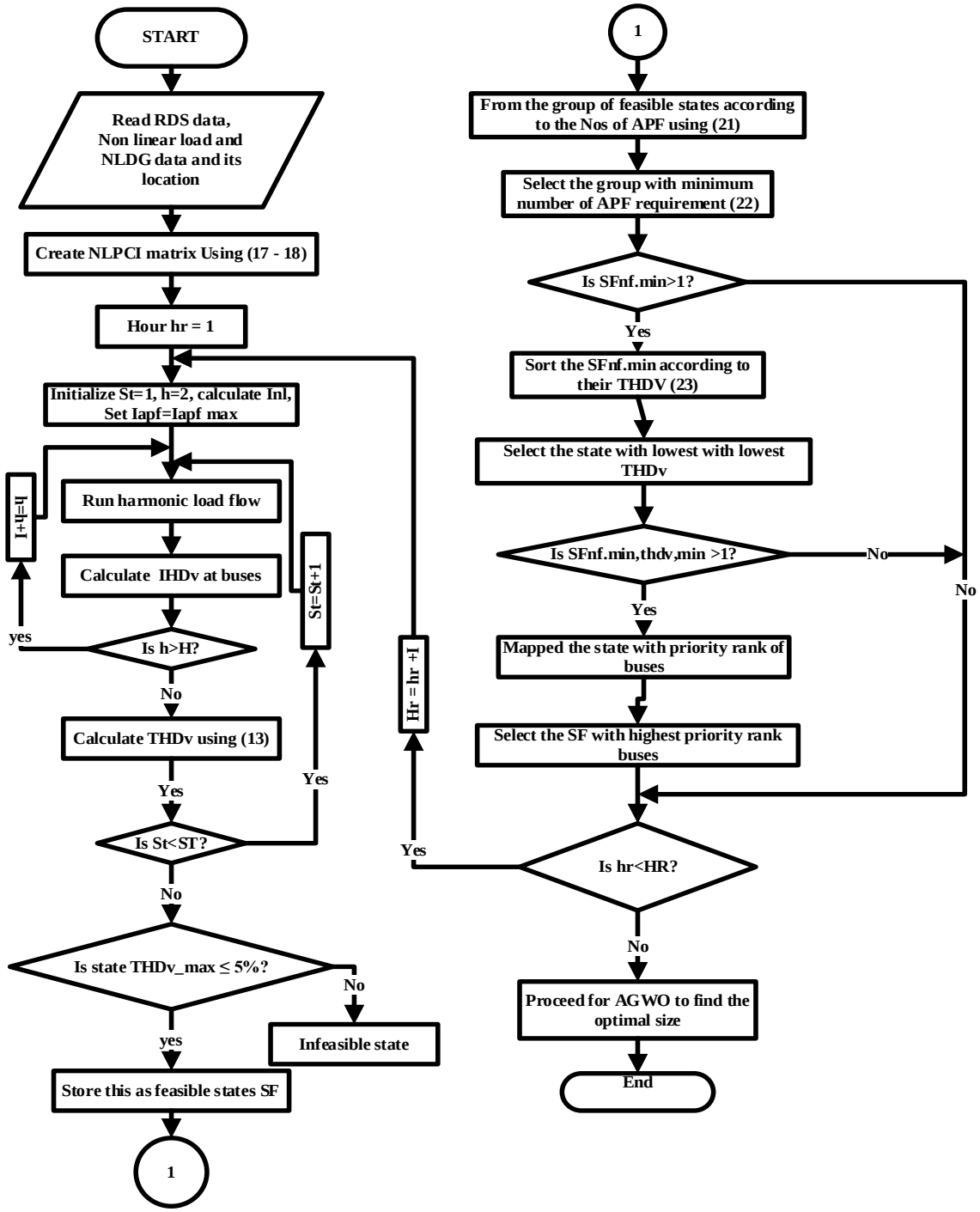

Figure 2: Flowchart for Extended NLPCI

Corresponding author's email address: muyik78@yahoo.com

2.9 Improved Aquila Algorithm

In 2021, Aquila Optimizer (AO), a population-based meta-heuristic algorithm was introduced by. The Latin word for eagles, or birds of prey, is Aquila. These birds are considered to be among the most cunning and proficient predators, possessing strong, sharpened claws and strapping feet that allow them to seize their prey with speed and agility (Lakum & Mahajan, 2019) . Aquila employs four main hunting techniques: strolling and capturing prey, contour flying with a brief glide, low flying with a slow drop, and high soar with a vertical stoop (Maya & Jasmin, 2017). These four core Aquila hunt mechanisms served as the inspiration for the creation of the AO, a nature-inspired optimization algorithm that fundamentally clarifies the actions of each hunt stage. initialization, expanded exploration, narrowed exploration, expanded exploitation, and narrowed exploitation are the five main processes that the traditional AO concentrates on. The first step taken in employing AO technique to address any problem is the initialization phase. Prior to initializing the other AO parameters, a random population of solutions will be formed. The broader exploration is step two, the expanded exploration essentially reveals the main hunting strategy used by the Aquila, which is a high ascent with a vertical stoop in which algorithms seek to determine the search pace from the high ascent. Equation (22) mathematically represents this strategy:

$$X_i(t+1) = X_{best}(t) \times \left(1 - \frac{t}{T}\right) + (X_M(t) - X_{best}(t) * rand) \quad 19$$

where $X_i(t+1)$ is the solution of the next iteration of t, and it is created by the first search technique. $X_{best}(t)$ is the finest solution found so far? $\left(1 - \frac{t}{T}\right)$ controls the exploration. T and t represent maximum number of iteration and current iteration respectively. X_M is the location mean value of current solution. Rand value lies between 0 to 1. X_M is calculated as follows (Abualigah):

$$X_M(t) = \frac{1}{N}\sum_{i=1}^{N} X_i(t) \quad 20$$

where N is the population size.

The third phase is narrowed exploration, the second hunting technique carried out by Aquila that is the contour flight with short glide is projected wherein Aquila approaches the land thereby circling around the target prey to attack. Such behavior of Aquila is precisely brought to light using Equation (21).

$$X_2(t+1) = X_{best}(t) \times Levy(D) + (X_R(t) + (y - x) * rand) \quad 21$$

where $X_2(t+1)$ denotes solution of the next iteration of t, X_{best} represents the best solution, $X_R(t)$ denotes the random solution belonging to N.

$$x = r \times \sin(\theta) \quad 22$$
$$y = r \times \cos(\theta) \quad 23$$

The improved Aquila optimization (IAO) algorithm is utilized in this work to improve the power quality of the system. The IAO is used to optimize the objective function. The IAO provides the variables to the system as input and observes the output. Current of APFs is taken as the input while the value of the objective function is taken as the output. The IAO then iteratively modifies the inputs of the system based on the feedbacks obtained until maximum number of iterations is met. The step-by-step procedure used in ensuring the improved algorithm properly places the APFs to achieve very minimal distortions as highlighted in the flowchart:

Corresponding author's email address: muyik78@yahoo.com

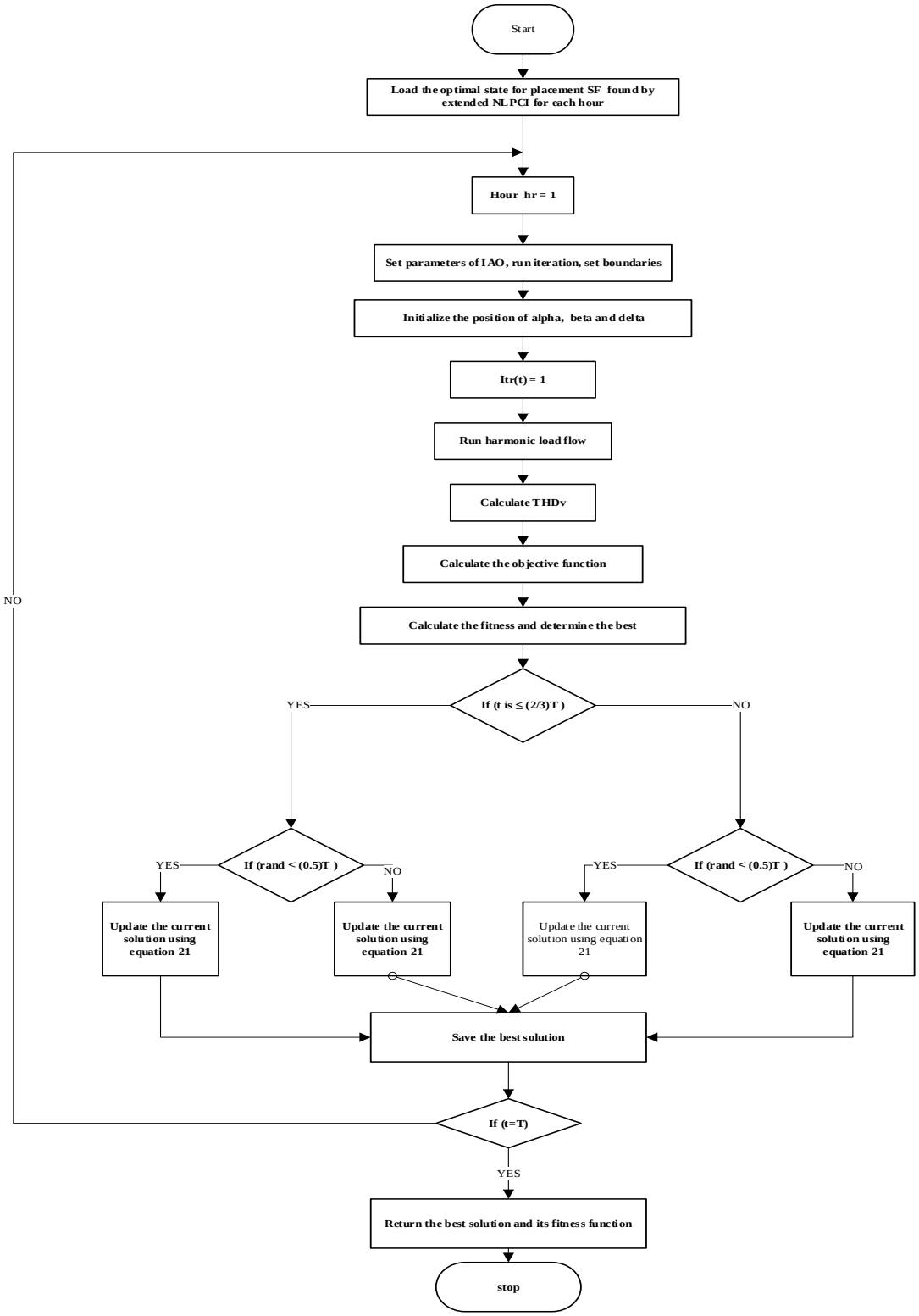

Figure 3: Flowchart of the Improved Aquila Algorithm

3. Results and Discussion

3.1 Convergence comparison between AGWO, AO and IAO

Figure 4 shows the convergence behavior of three optimization algorithms AGWO, IAO, AO over a specified number of iterations. All three algorithms demonstrate rapid improvement in fitness during the initial 20 iterations, indicating their ability to explore the solution space effectively at the beginning of the optimization process. Among the three, IAO shows a steeper drop in fitness compared to AGWO and AO during the early iterations, suggesting a faster convergence rate in the initial stages. Between iterations 20 to 40, the algorithms continue to refine the fitness values. IAO converges faster than AGWO and AO during this phase, reaching near-optimal fitness earlier than the other two algorithms performs slightly better than AO in reducing the fitness value during this phase. By iteration 40, AO reaches a stable fitness value, plateauing earlier than the

Corresponding author's email address: muyik78@yahoo.com

other algorithms. IAO achieves the best (lowest) fitness value overall, demonstrating superior accuracy and convergence speed. AGWO converges slightly later than IAO but reaches a comparable fitness level, outperforming AO in terms of final solution quality. IAO achieves the best final fitness value, fastest convergence, and most stable performance, indicating its efficiency and robustness. AGWO offers competitive performance, converging to a fitness level close to IAO but requiring more iterations. AO converges the earliest but stabilizes at a higher fitness value, suggesting it might be prone to premature convergence or local optima.

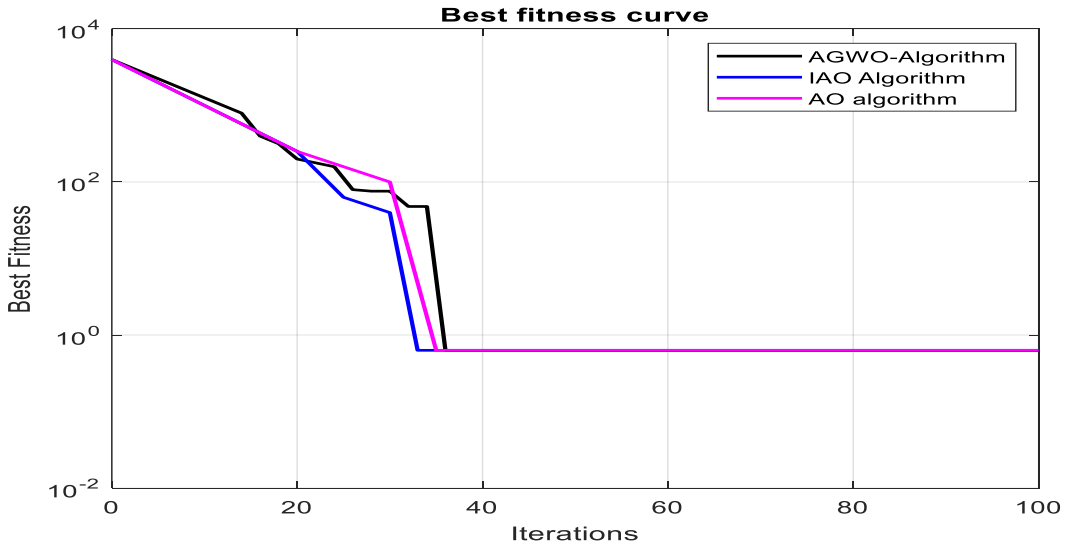

Figure 4: Iteration curve for IAO, AO and AGWO

3.2 Comparison of AGWO with and without APF

The bar graph in Figure 5 shows a comparative analysis of AGWO with APF and without APF across some buses. THDv values are generally lower when the Active Power Filter (APF) is employed (orange bars) compared to when it is not (blue bars). This indicates the effectiveness of APF in reducing harmonic distortion. THDv increases significantly at certain bus numbers, such as buses around 20, 30, and 70. These buses may represent areas of the network with higher harmonic contributions due to nonlinear loads or other factors. At most buses, the addition of APF (orange bars) reduces THDv, but the reduction is more prominent in areas with higher harmonic distortion (bus 26). At bus 26, the highest THDv is observed, both with and without APF. However, the reduction in THDv with APF is notable, showing the APF's ability to mitigate harmonics in heavily distorted areas. The effect of APF is less prominent in buses with inherently lower THDv. The graph highlights the importance of APF in reducing harmonic distortions, especially in buses with significant harmonic contributions. This is critical for maintaining power quality in the system.

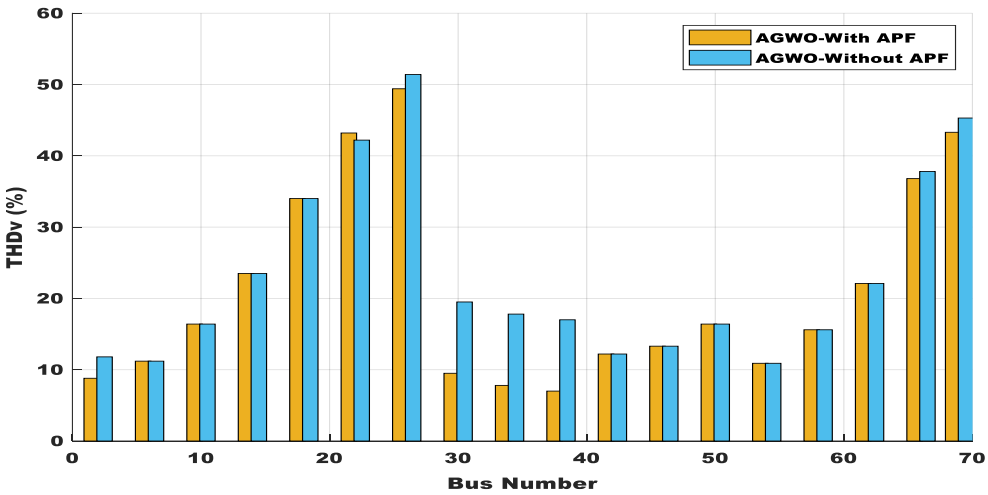

Figure 5: Comparison of AGWO with APF and without APF

Corresponding author's email address: muyik78@yahoo.com

3.3 Comparison of AO with APF and without APF

Figure 6 compares the THDv across bus numbers in a power distribution system under two conditions i.e. AO without APF and AO with APF. The THDv values are consistently lower with the APF compared to without the APF, demonstrating the effectiveness of the APF in reducing harmonic distortion. This reduction is more prominent at buses with higher THDv values, such as bus numbers 22, 26, 30, and 69**.** Bus 26 shows the highest THDv in the system without APF. With the APF in place, there is a significant reduction in THDv, highlighting the APF's effectiveness in heavily distorted regions. Bus 30 and Bus 66 similarly experience high THDv values without APF. The addition of the APF results in noticeable improvements. At buses with moderate THDv values (bus 10, 14, and 62), the reduction is less but still consistent. At buses with low THDv (bus 2, 6, and 34), the APF has minimal impact, as the distortion is already within acceptable limits. This indicates that these areas may not require intensive harmonic mitigation.AO technique is effective in identifying optimal placement or configuration of APFs. This is evident from the consistent reduction in THDv across the network that AO-optimized APF performs well in areas of high distortion. AO seems to result in a more even reduction across the network, while AGWO's performance appeared more focused on critical areas.

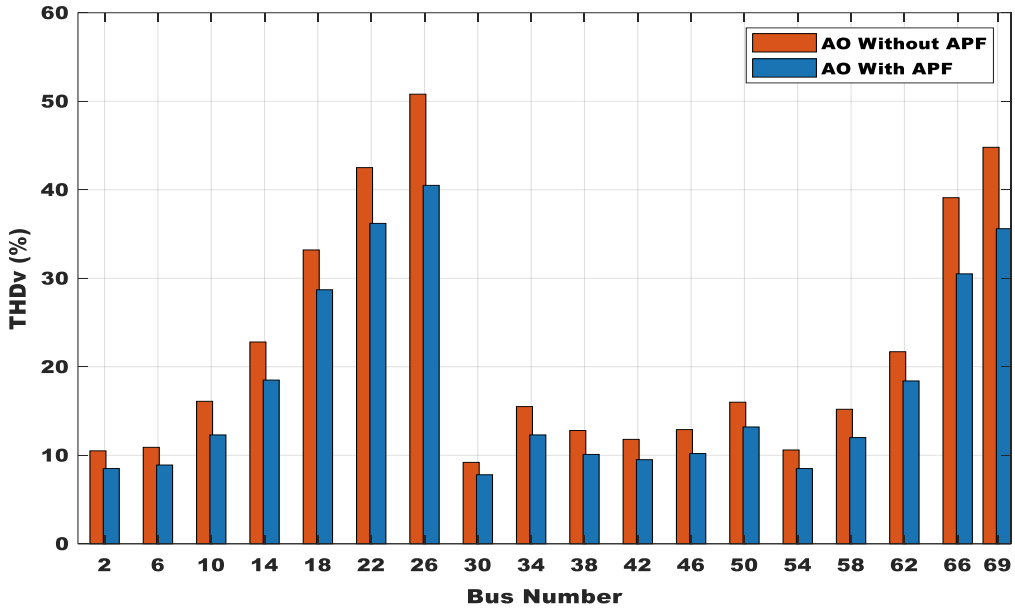

Figure 6: Comparison of AO with and without APF

3.4 Comparison of IAO with and without APF

Figure 7 presents the THDv across bus numbers in a power distribution using IAO without APF and IAO with APF**.** THDv values are consistently lower with APF compared to without APF (darker green), demonstrating the effectiveness of the APF in mitigating harmonics when optimized using the IAO. Bus 26 experiences the highest THDv without APF. With APF, there is a significant reduction, showing the optimization and mitigation strategy's effectiveness at this critical node. Buses 22, 30, and 66 also show substantial reductions in THDv with the inclusion of APF. However, bus 66 still retains a relatively high THDv even with the APF. At buses with low inherent THDv, such as buses 2, 6, and 34, the APF has a minimal effect, as the harmonic distortion is already within acceptable limits. Without APF, there are multiple buses (22, 26, 30, and 66) where THDv exceeds 40%. After deploying the APF, these values drop significantly, indicating that IAO effectively prioritizes the buses with the highest distortion during optimization. The IAO-optimized APF achieves substantial harmonic mitigation across the network. The graph demonstrates that IAO effectively reduces THDv at critical buses (26, 30) while maintaining reasonable computational efficiency. Compared to AGWO and AO (based on earlier graphs). IAO shows comparable performance in terms of THDv reduction, especially at high-distortion buses. The improved optimization capability of IAO likely leads to better placement and tuning of APFs, especially in areas with higher harmonic contributions. The algorithm's enhanced exploration and exploitation features might result in a more balanced THDv reduction across the network.

Corresponding author's email address: muyik78@yahoo.com

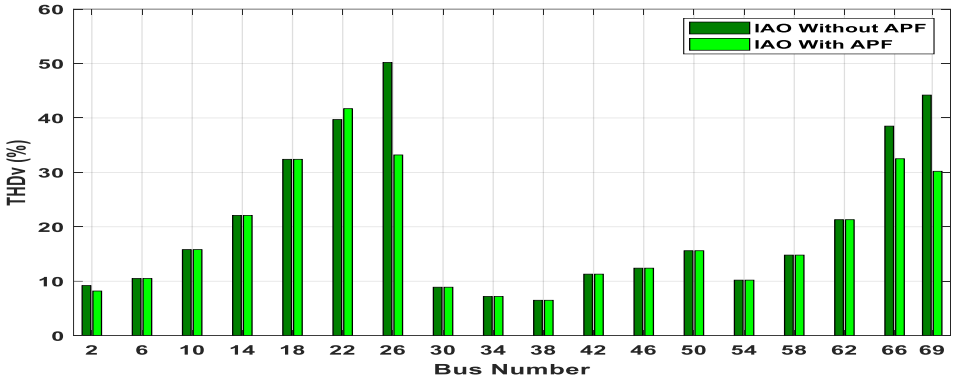

Figure 7: Comparison of IAO with and without APF

3.5 Comparison between AGWO, AO and IAO with APF from 7-12

Table 1 compares the THD percentage across different bus numbers in a power distribution network for three optimization methods i.e. AGWO, AO, and IAO. THD varies significantly across bus numbers, with higher values observed at certain buses, indicating areas with more pronounced harmonic distortion. The highest THD is observed in the upper bus numbers (69th bus), where the impact of nonlinear loads might be more severe. IAO consistently achieves the lowest THD across most buses, indicating its superior performance in mitigating harmonic distortion when using APF. AGWO shows moderate performance, performing better than AO at most buses but worse than IAO. The AO tends to have higher THD compared to the other two methods, suggesting it may be less effective in optimizing APF parameters. The values of the harmonic distortion at all the buses is shown in Table 1 for hour 12. This time is chosen for this research because, THDv is observed to be higher at this particular time compared to other period.

Table 1: Comparative Values of THDi pu from 7th to 12th hours

Hour	AGWO	AOQ	IAOQ
7th	0.01	0.01	0.01
8th	0.23	0.06	0.05
9th	0.40	0.22	0.21
10th	0.55	0.36	0.35
11th	0.61	0.53	0.51
12th	0.67	0.60	0.58

3.6 Comparison between AGWO, AO and IAO without APF

Figure 8 displays a comparison of voltage total harmonic distortion (THD) across (numbered 1 through 70, with increments of 4) for three different optimization algorithms: AGWO, AO, and IAO. The AGWO-With APF is represented by the blue bars, AO-With APF by the orange bars, and IAO-With APF by the yellow bars. The 'APF' in the legend stands for Active Power Filter, which is used to reduce harmonic distortion. The vertical axis, labeled THD (%), represents the voltage total harmonic distortion as a percentage. THD is a measure of the harmonic content in the voltage waveform, indicating how much the voltage deviates from a pure sine wave. Lower values are desirable as they signify a cleaner, more stable power supply with less distortion. The horizontal axis is labeled Bus Number, representing different points in an electrical system. The IAO consistently shows the lowest THD values across all the buses compared to the other two algorithms. This suggests that the IAO algorithm is the most effective at minimizing voltage distortion under the tested conditions. While the IAO algorithm is generally the best performer, the AGWO and AO algorithms have similar THD values for many buses. The highest THD values, exceeding 50% at bus 26, indicating a significant level of voltage distortion at that specific point in the system. The IAO algorithm still manages to perform slightly better at this point with a value of 50.2%. Table 2 shows a summary of the comparison of the 3 algorithms without APF.

3.7 Comparison between AGWO, AO and IAO with APF

Figure 9 compares the performance of three optimization algorithms, AO, and IAO in reducing voltage total harmonic distortion. IAO algorithm consistently achieves the lowest THD values across all the buses shown. This indicates that the IAO algorithm is the most effective of the three at minimizing voltage distortion. The

performance of the AGWO and AO algorithms is very similar. For many buses, the orange bar (AO) is barely visible because it is almost entirely covered by the yellow bar (AGWO), which has a slightly higher THD$_{v}$. Both perform worse than the IAO algorithm in most cases. The highest THD values for all three algorithms are observed at Bus 26 and Bus 69. However, even at these points of high distortion, the IAO algorithm still maintains a significantly lower THD compared to the other two. Table 3 shows a summary of the comparison of the 3 algorithms with APF.

Table 2: Summary of comparison between IAO, AO and AGWO without APF

Bus No	IAO	AO	AGWO (%)	AO (%)	AGWO (%)
2	9.2	10.5	11.8	12.38	22.03
6	10.5	10.9	11.2	3.67	6.25
10	15.8	16.1	16.4	1.86	3.66
14	22.1	22.8	23.5	3.07	5.96
18	32.4	33.2	34	2.41	4.71
22	39.7	42.5	42.2	6.59	5.92
26	50.2	50.8	51.4	1.18	2.33
30	8.9	9.2	19.5	3.26	54.36
34	7.2	15.5	17.8	53.55	59.55
38	6.5	12.8	17	49.22	61.76
42	11.3	11.8	12.2	4.24	7.38
46	12.4	12.9	13.3	3.88	6.77
50	15.6	16	16.4	2.50	4.88
54	10.2	10.6	10.9	3.77	6.42
58	14.8	15.2	15.6	2.63	5.13
62	21.3	21.7	22.1	1.84	3.62
66	37.8	38.5	39.7	1.82	4.79
69	44.2	44.8	45.3	1.34	2.43

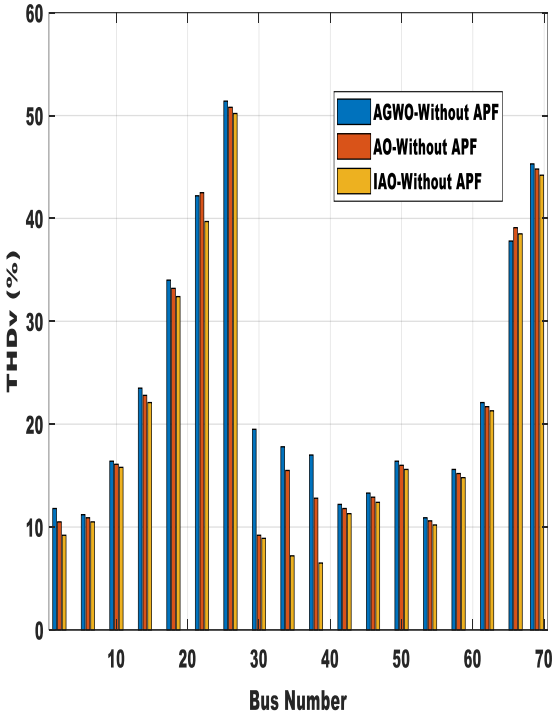

Figure 8: Comparison between IAO, AO and AGWO without APF

Table 3: Summary of comparison between IAO, AO and AGWO with APF

Bus No	IAO	AO	AGWO	AO (%)	AGWO (%)
2	8.2	8.5	8.8	3.53	6.82
6	10.5	10.9	11.2	3.67	6.25
10	15.8	16.1	16.4	1.86	3.66
14	22.1	22.8	23.5	3.07	5.96
18	32.4	33.2	34	2.41	4.71
22	41.7	42.5	43.2	1.88	3.47
26	33.2	48.8	49.4	31.97	32.79
30	8.9	9.2	9.5	3.26	6.32
34	7.2	7.5	7.8	4.00	7.69
38	6.5	6.8	7	4.41	7.14
42	11.3	11.8	12.2	4.24	7.38
46	12.4	12.9	13.3	3.88	6.77
50	15.6	16	16.4	2.50	4.88
54	10.2	10.6	10.9	3.77	6.42
58	14.8	15.2	15.6	2.63	5.13
62	21.3	21.7	22.1	1.84	3.62
66	32.5	39.1	36.8	16.88	11.68
69	30.2	40.8	43.3	25.98	30.25

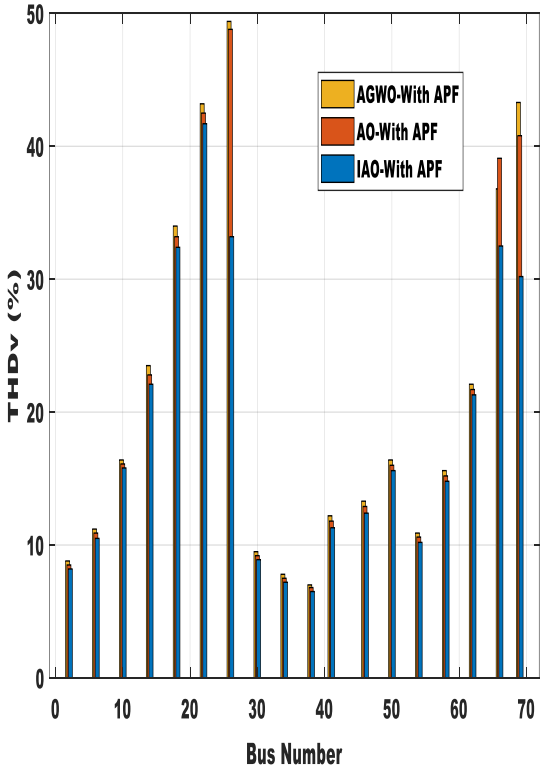

Figure 9: Comparison between IAO, AO and AGWO with APF

Corresponding author's email address: muyik78@yahoo.com

4. Conclusion

This paper developed and implemented an improved Aquila Optimizer-based Distributed Generation (DG) system for mitigating harmonics in a radial distribution network (RDN). By integrating nonlinear loads (NLLD) and nonlinear distributed generation (NLDG) into the model, the study effectively addressed real-world harmonic distortion issues commonly found in power systems. The improved Aquila Optimization (IAO) algorithm demonstrated superior capability in optimally sizing and placing Active Power Filters (APFs) within the RDN to ensure compliance with the IEEE-519 (1992) harmonic distortion limits. Simulation results carried out in the MATLAB/Simulink R2022b environment confirmed the robustness and accuracy of the developed scheme. The improved algorithm achieved significant reductions in Total Harmonic Distortion (THD) across the IEEE 69-bus system, particularly during high distortion periods between 11:00 and 13:00 hours. Comparative analysis showed that the proposed IAO-based method consistently outperformed both the Adaptive Grey Wolf Optimizer (AGWO) and the standard Aquila Algorithm (AO), achieving THD reductions of up to 32.79% and 31.97%, respectively, at the most distorted buses. Overall, the results validate the efficiency and reliability of the improved Aquila Optimizer in enhancing power quality and maintaining voltage stability in distribution networks. The developed approach provides a practical and computationally efficient solution for harmonic mitigation and can be extended to larger and more complex power systems for improved grid performance.

References

Abbas, AS., El-Sehiemy, RA., Abou El-Ela, A., Ali, ES., Mahmoud, K., Lehtonen, M., & Darwish, MMF. 2021. Optimal harmonic mitigation in distribution systems with inverter based distributed generation. *Applied Sciences (Switzerland)*, *11*(2): 1–16. https://doi.org/10.3390/app11020774

Battu, NR., Abhyankar, AR., & Senroy, N. 2015. DG planning with amalgamation of economic and reliability considerations. *International Journal of Electrical Power and Energy Systems*, *73*, 273–282. https://doi.org/10.1016/j.ijepes.2015.05.006

Çiçek, A., Erenoğlu, A. K., Erdinç, O., Bozkurt, A., Taşcıkaraoğlu, A., & Catalão, J. P. S. 2021. Implementing a demand side management strategy for harmonics mitigation in a smart home using real measurements of household appliances. *International Journal of Electrical Power and Energy Systems*, *125*(December 2019). https://doi.org/10.1016/j.ijepes.2020.106528

Dhal, K. G., Das, A., Sasmal, B., Ghosh, T. K., & Sarkar, K. 2024. Eagle Strategy in Nature-Inspired Optimization: Theory, Analysis, Applications, and Comparative Study. *Archives of Computational Methods in Engineering*, *31*(3), 1213–1232. https://doi.org/10.1007/s11831-023-10014-1

Fahmi, M. I., Baafai, U., Hazmi, A., & Nasution, T. H. 2018. Harmonic reduction by using single-tuned passive filter in plastic processing industry. *IOP Conference Series: Materials Science and Engineering*, *308*(1). https://doi.org/10.1088/1757-899X/308/1/012035

Lakum, A., & Mahajan, V. 2019. Optimal placement and sizing of multiple active power filters in radial distribution system using grey wolf optimizer in presence of nonlinear distributed generation. *Electric Power Systems Research*, *173*(September 2018), 281–290. https://doi.org/10.1016/j.epsr.2019.04.001

Lakum, A., & Mahajan, V. 2021. Engineering Science and Technology , an International Journal A novel approach for optimal placement and sizing of active power filters in radial distribution system with nonlinear distributed generation using adaptive grey wolf optimizer. *Engineering Science and Technology, an International Journal*, *24*(4), 911–924. https://doi.org/10.1016/j.jestch.2021.01.011

Maya, K. N., & Jasmin, E. A. 2017. Optimal integration of distributed generation (DG) resources in unbalanced distribution system considering uncertainty modelling. *International Transactions on Electrical Energy Systems*, *27*(1). https://doi.org/10.1002/etep.2248

Mirjalili, S., & Lewis, A. 2016. The Whale Optimization Algorithm. *Advances in Engineering Software*, *95*, 51–67. https://doi.org/10.1016/j.advengsoft.2016.01.008

Corresponding author's email address: muyik78@yahoo.com

Owosuhi, A., Hamam, Y., & Munda, J. 2024. A New Framework for Active Loss Reduction and Voltage Profile Enhancement in a Distributed Generation-Dominated Radial Distribution Network. *Applied Sciences (Switzerland)*, *14*(3). https://doi.org/10.3390/app14031077

Sakar, S., Balci, M. E., Abdel Aleem, S. H. E., & Zobaa, A. F. 2017. Increasing PV hosting capacity in distorted distribution systems using passive harmonic filtering. *Electric Power Systems Research*, *148*, 74–86. https://doi.org/10.1016/j.epsr.2017.03.020

Uniyal, A., & Kumar, A. 2018. Optimal Distributed Generation Placement with Multiple Objectives Considering Probabilistic Load. *Procedia Computer Science*, *125*(2017), 382–388. https://doi.org/10.1016/j.procs.2017.12.050

Vinayagam, A., Aziz, A., PM, B., Chandran, J., Veerasamy, V., & Gargoom, A. 2019. Harmonics assessment and mitigation in a photovoltaic integrated network. *Sustainable Energy, Grids and Networks*, *20*, 100264. https://doi.org/10.1016/j.segan.2019.100264

Corresponding author's email address: muyik78@yahoo.com